

DYNAMICS AND STRENGTH OF METAL-COMPOSITE CYLINDERS ON INTERNAL EXPLOSION AGAINST THE THICKNESS AND PROPERTIES OF METALLIC AND COMPOSITE LAYERS. PART 1. NUMERICAL SIMULATION OF THIN- AND MEDIUM-THICKNESS CYLINDERS

P. P. Lepikhin, V. A. Romashchenko, S. O. Tarasovska,¹
and O. S. Beiner

UDC 539.4

The effect of the metallic layer thickness on the stress-strain state and strength of metal-composite cylinders of the total constant thickness under internal dynamic pressure produced by the explosion of a charge evenly distributed along its axis in air at the constant total-to-running charge mass ratio $\xi = 1.421$ mm was numerically investigated. The strength of the cylinders was evaluated by the generalized Mises criterion. The strength of shells with a unidirectionally circularly reinforced outer composite layer for the composites of low tensile strength in the isotropy plane is shown to be mainly governed by the wave processes across the shell width. Under this condition, its dependence on radial and axial stresses is much higher than on the circumferential ones, which are usually much larger than the first two components of the stress tensor. The four composites and two designs of the cylinders: thin-walled and medium-thickness are examined. The cylinders are double-layered: the inner layer is steel (St20) and the outer layer is a circularly reinforced composite. At given ξ and the total constant cylinder thickness H , the optimum in strength terms ratio β_{opt} of the metallic layer thickness h to H is strongly dependent on H , a composite (i.e., its physico-mechanical characteristics) and varies within 0.4–0.7 for thin-walled cylinders and 0.6–0.7 for medium-thickness ones. Irreversible plastic energy losses in the inner steel layer have a significant impact on the shell strength, as a result the shock wave travelling to the outer composite layer is of lower intensity and the strength of the object as a whole can be ensured. The inclusion of the plastic steel layer deformation in thin-walled cylinder calculations significantly changes the dynamics of objects qualitatively but insignificantly increases the strength quantitatively, the Mises strength function can be reduced by less than 5% compared to an ideally elastic calculation. If the plastic metal deformation is accounted for medium-thickness cylinders, it significantly changes the wave patterns both qualitatively and quantitatively, the strength function can be reduced by almost 50% compared to the elastic calculation.

Keywords: metal-composite cylinder, internal explosive loading, unidirectionally reinforced composite layer, strength, stress-strain state, numerical methods.

Introduction. The dynamic stress-strain state and strength of hollow multilayer wound rotational metal-composite (MC) shells on the internal explosion of a spherical charge in air are little investigated, with a small number of theoretical and experimental studies devoted this problem. The literature review is given in the previous paper of the authors [1], there it is noted that to date, the thickness of elastoplastic metal layers and the mechanical characteristics of composite layers that provide the best carrying capacity of MC cylinders under internal explosive loading have not been determined.

Pisarenko Institute of Problems of Strength, National Academy of Sciences of Ukraine (¹tsa@ipp.kiev.ua).
Translated from Problemy Mitsnosti, No. 6, pp. 33 – 45, November – December, 2022. Original article submitted September 28, 2022.

The one-dimensional dynamic stress-strain state and strength of wound MC cylinders were numerically studied and the thickness of elastoplastic metallic layers that provide the highest carrying capacity of cylinders under internal explosive loading in air was evaluated in [1]. At the same time, only one specific composite was studied as the outer layer of the MC cylinder. This investigation is going on with a study [1] to determine the optimum thickness in terms of strength for elastoplastic metallic layers and mechanical characteristics of composite layers from four different composites. As in [1], the explosive loading is simulated using the CONWEP program [2, 3] and the generalized Mises strength criterion [4], the simplest of the Tsai–Wu ones, is correct (i.e., satisfies the necessary and sufficient conditions for the strength surface existence), it can also adequately assess the composite strength at the lowest costs spent for criterial experiments.

The object of the study is: to numerically investigate the strengthening behavior of an MC cylindrical double-layer (metal–composite) shell of the total constant thickness H under internal dynamic pressure from the explosion of a spherical charge located in the center of cylinder symmetry at the constant total-to-running charge mass ratio, to identify the best thicknesses of metallic layers and physicommechanical characteristics of composites that provide the highest carrying capacity of the double-layer MC cylinder. The inner layer is isotropic elastoplastic steel, and the outer layer is a circularly reinforced cylindrically transtropic elastic composite. The dynamic problem is solved in the 1D statement of the plane strain state at the cylinder ends to obtain the most qualitative and illustrative results.

Mathematical Formulation and Solution Method. Consider the plane strain state of a double-layer cylinder under axisymmetric internal dynamic pressure from the explosion of a charge evenly distributed lengthwise and located in line with the axis of symmetry. In this case, the pressure pulse corresponds to the explosion of a spherical charge of a certain mass M in air at a distance equal to the inner radius of the cylinder. The inner layer is isotropic elastoplastic steel of full strength in tension–compression (the equations of the Prandtl–Reuss nonhardening material flow theory were used [5]). The outer layer is a circularly reinforced cylindrically transtropic fully elastic composite of unequal tensile–compression strength with the ideal layer-to-layer contact. The problem is numerically solved by the finite difference method (FDM) in the cylindrical Eulerian coordinates x, φ, r , in view of the axial symmetry and plane strain state on any end planes $x = \text{const}$. The finite-difference Lagrangian mesh is frozen in the medium and moves in space and time with it. Thus, we have the computational domains for the 1D problem: $R \leq r \leq R + h$ for the inner and $R + h \leq r \leq R + H$ for the outer layers of the cylinder, where R is the inner radius of the inner cylinder, h is the thickness of the inner steel layer, H is the total thickness of the cylinder, and $H - h$ is the thickness of the outer composite layer. The complete system of differential equations together with initial, boundary, and contact conditions is given in [1].

The strength of a double-layer cylinder is estimated by the generalized Mises criterion [4], which for a circularly reinforced cylindrically transtropic composite at the plane strain state is as follows:

$$\Phi = (\sigma_x + \sigma_r) \left(\frac{1}{\sigma_+} - \frac{1}{\sigma_-} - \frac{\sigma_\varphi}{\sqrt{\sigma_{\varphi+}\sigma_{\varphi-}\sigma_+\sigma_-}} \right) + \sigma_\varphi \left(\frac{1}{\sigma_{\varphi+}} - \frac{1}{\sigma_{\varphi-}} \right) + \frac{\sigma_x^2 + \sigma_r^2 - \sigma_x\sigma_r}{\sigma_+\sigma_-} + \frac{\sigma_x^2}{\sigma_{\varphi+}\sigma_{\varphi-}} < 1, \quad (1)$$

where $\sigma_{\varphi+}$ and $\sigma_{\varphi-}$ are the ultimate strengths of the circular reinforcement direction in tension–compression, respectively, σ_+ and σ_- are the same in the isotropy plane xr ($\varphi = \text{const}$), Φ is the strength function, and $\sigma_x, \sigma_r, \sigma_\varphi$ are the stress tensor components. If (1) is fulfilled, the strength is maintained. Otherwise, ($\Phi \geq 1$), the strength criterion is not satisfied, and the material is fractured in this point. The cases of isotropic and/or materials of full strength in tension–compression are easily obtained from (1) as partial (degenerate). Note that in all further calculations, the inner (first) layer is made of isotropic steel of full strength in tension–compression and for it, the Mises criterion (1) degenerates into the classical fourth theory of strength [6].

The dynamic 1D boundary problem is numerically solved with the application package earlier developed by the authors [7]. The solution method is the Wilkins time-explicit finite-difference integro-interpolation algorithm [8], modified by the authors for anisotropic materials and included in this package. The strength, i.e., Φ function, is

calculated at each time step in each finite-difference element of the computational domain. If its maximum value over the entire volume of the computational domain Φ_{max} was less than unity, the object was recognized as strong; otherwise, the strength of the cylinder as a whole was believed to be deteriorated, and the failure was recorded.

Materials. The inner layer is isotropic elastoplastic St20 steel of full strength in tension–compression with the physico-mechanical characteristics [6]: density $\rho = 7860 \text{ kg/m}^3$, Young's modulus $E = 212000 \text{ MPa}$, Poisson's ratio $\nu = 0.3$, yield strength $\sigma_Y = 250 \text{ MPa}$, and $\sigma_+ = \sigma_- = \sigma_u = 420 \text{ MPa}$.

The outer layer is a cylindrically transropic circularly reinforced elastic composite of unequal tensile–compression strength. The four composites were examined:

C No. 1: T300/5208 graphite epoxy with the volume fiber content $V = 70\%$ and physico-mechanical characteristics [9]: $\rho = 1583 \text{ kg/m}^3$, $E = 14,900 \text{ MPa}$, $\nu = 0.386$, $E_\varphi = 162,000 \text{ MPa}$, $\nu_\varphi = 0.283$, $\sigma_+ = 52.6 \text{ MPa}$, $\sigma_- = 260 \text{ MPa}$, $\sigma_{\varphi+} = 1744 \text{ MPa}$, and $\sigma_{\varphi-} = 1650 \text{ MPa}$. Here, E_φ is Young's modulus in the circumferential direction, ν_φ is Poisson's ratio corresponding to the circumferential direction [1, 4, 10].

C No. 2: T300/5208 graphite epoxy with the volume fiber content $V = 40\%$ and physico-mechanical characteristics [9]: $\rho = 1406 \text{ kg/m}^3$, $E = 7900 \text{ MPa}$, $\nu = 0.436$, $E_\varphi = 94,100 \text{ MPa}$, $\nu_\varphi = 0.309$, $\sigma_+ = 49.5 \text{ MPa}$, $\sigma_- = 220 \text{ MPa}$, $\sigma_{\varphi+} = 1013 \text{ MPa}$, and $\sigma_{\varphi-} = 940 \text{ MPa}$.

C No. 3: E-glass epoxy with the volume fiber content $V = 65\%$ and physico-mechanical characteristics [9]: $\rho = 2112 \text{ kg/m}^3$, $E = 15,300 \text{ MPa}$, $\nu = 0.332$, $E_\varphi = 48,000 \text{ MPa}$, $\nu_\varphi = 0.315$, $\sigma_+ = 27.8 \text{ MPa}$, $\sigma_- = 150 \text{ MPa}$, $\sigma_{\varphi+} = 1297 \text{ MPa}$, and $\sigma_{\varphi-} = 820 \text{ MPa}$.

C No. 4: E-glass epoxy with the volume fiber content $V = 40\%$ with physico-mechanical characteristics [9]: $\rho = 1750 \text{ kg/m}^3$, $E = 8300 \text{ MPa}$, $\nu = 0.395$, $E_\varphi = 30,900 \text{ MPa}$, $\nu_\varphi = 0.327$, $\sigma_+ = 27.1 \text{ MPa}$, $\sigma_- = 140 \text{ MPa}$, $\sigma_{\varphi+} = 798 \text{ MPa}$, and $\sigma_{\varphi-} = 480 \text{ MPa}$.

For convenience and shortening the text, the composites to be calculated will be specified by the above numbers.

Object Geometry. The inner radius R of the cylindrical MC shell remained constant in all calculations, viz $R = 150 \text{ mm}$. The three versions of MC double-layer shells classified under their total thickness H are examined:

- (i) thin: $H = 10 \text{ mm}$, $H/R = 0.067$;
- (ii) medium thickness: $H = 20 \text{ mm}$, $H/R = 0.133$;
- (iii) thick: $H = 40 \text{ mm}$, $H/R = 0.267$.

The thickness of the inner steel layer h varied within $(0-0.8)H$. Thus, the thickness ratio of the metal $\beta = h/H$ varied within $0-0.8$. At $\beta = 0$, we have a single-layer composite shell; at $\beta > 0$, we have a double-layer MC shell. There was no point to discuss the $\beta > 0.8$ cases as unattractive in terms of their practical application.

Loading. As in [1], the explosive charge mass in the TNT equivalent M was dependent on H and β so that the mass ratio $\xi = M/m$ remained constant for each of the three shell versions. Here, m is the running mass (per unit length) of the shell:

$$m = \pi\pi H[\rho_m\beta(2R + \beta H) + \rho_c(1 - \beta)(2R + H + \beta H)], \quad (2)$$

where ρ_m is the metal density and ρ_c is the composite density.

Thus, $M(\beta)$ in each case was calculated by the formula

$$M(\beta) = \xi m, \quad (3)$$

where $m(\beta, H)$ is determined from (2).

Hereinafter ξ is constant and equal to $\xi = 1.421 \text{ mm} = \text{const}$. The M calculations were carried out by scheme (2)–(3). Since the 3 H values (10, 20, and 40 mm), the 4 composites (ρ_c discretely varied from 1406 to 2112 kg/m^3) and a wide β interval ($0-0.8$) were discussed, the charge mass M was also examined over a fairly wide range, from

19.46 g for the thin-walled ($H = 10$ mm) single-layer ($\beta = 0$) composite cylinder [C No. 2] to 400.86 g for the thick-walled ($H = 40$ mm) double-layer ($\beta = 0.8$) MC cylinder [St20; C No. 3].

Finite-Difference Mesh Parameters. With the application package [7], the mesh step along the radial coordinate was constant and equal to $dr = 0.1$ mm. This ensured sufficient and equal calculation accuracy for all three shell versions. Thus, at $H = 10, 20,$ and 40 mm, the cylinder was partitioned across its width into 100, 200, and 400 finite-difference elements, respectively. The contact surface should always coincide with the node of the computational domain, so the thickness h of the inner steel layer could discretely change with the step $dr = 0.1$ mm. The time step was chosen automatically subject to the Kurant stability condition. The calculations were carried out to the point in time of 100–200 μ s to fit H and β values and cover the first half-period of radial shell vibrations, the most dangerous in terms of strength [4]. If the dynamics (vibrations) of cylinders in a wider time range were of interest, some calculations were sometimes performed on a half as fine (and more accurate) finite-difference mesh with $dr = 0.05$ mm. Hereinafter the notation is adopted: Φ_{maxc} is the maximum value of the Mises strength function Φ , which is achieved across the whole width of the outer composite layer at the first half-period of radial vibrations for the total calculated time interval t_{calc} , i.e., the global Φ maximum in the open rectangle ($R + h < r < R + H; 0 < t < t_{calc}$).

Numerical Results.

Thin-Walled Cylinders.

Determination of Optimum β (hereafter β_{opt}) and an Outer Composite Layer of Optimum Strength. Thin-walled ($H = 10$ mm; $H/R = 10/150 = 0.0667$) double-layer MC cylinders [St20; C] were examined for four outer composite layers and nine β values, from 0 to 0.8 with a step of 0.1 (at $\beta = 0$, we have single-layer composite cylinders). The data obtained were used to plot Fig. 1, where the solid, dashed, dot-and-dash, and dotted curves correspond to the MC cylinders of [St20; C No. 1], [St20; C No. 2], [St20; C No. 3], and [St20; C No. 4], respectively. As is seen, the MC cylinders [St20; C No. 1] and [St20; C No. 2] are of higher strength than [St20; C No. 3] and [St20; C No. 4]. Even single-layer ($\beta = 0$) shells [C No. 1] and [C No. 2] possessed quite a high safety margin in contrast to similar [C No. 3] and [C No. 4]. At the same time, if the MC cylinder [St20; C No. 3] started to satisfy the strength condition already at $\beta \geq 0.02$, [St20; C No. 4] only at $\beta > 0.3$. The MC cylinders [St20; C No. 2] were found to be of the highest strength, while [St20; C No. 3] were the most dangerous. Although the corresponding strength limits in C No. 1 are higher than those in C No. 2, and those in C No. 3 are higher than those in C No. 4, the MC cylinders [St20; C No. 2] are stronger than [St20; C No. 1], and [St20; C No. 4] are stronger than [St20; C No. 3]. The reason is that the strength of such composites under explosive loading is primarily determined by the tensile strength σ_+ in the isotropy plane, i.e., in the radial (r) and axial (x) directions. With an increase in the volume content V of reinforcing fibers from 40 to 70% in C No. 1 compared to C No. 2 and from 40 to 65% in C No. 3 compared to C No. 4, these strength limits increased insignificantly compared to the density of the composites. Therefore, at fixed ξ , the growth of the mass M of the explosive charge will occur faster than the growth of the corresponding strength limits σ_+ , and thus, the strength of the MC cylinder will decrease.

From Fig. 1, determine the optimum thickness ratio β_{opt} of the steel layer in which the corresponding Φ_{maxc} are minimum:

for MC shell [St20; C No. 1] $\beta_{opt} = 0.4$; $\Phi_{maxc}(\beta_{opt}) = \min = 0.2138 \ll 1$;

for [St20; C No. 2] $\beta_{opt} = 0.5$; $\Phi_{maxc}(\beta_{opt}) = \min = 0.1988 \ll 1$;

for [St20; C No. 3] $\beta_{opt} = 0.7$; $\Phi_{maxc}(\beta_{opt}) = \min = 0.7072 < 1$;

for [St20; C No. 4] $\beta_{opt} = 0.7$; $\Phi_{maxc}(\beta_{opt}) = \min = 0.4176 \ll 1$.

The composite of optimum strength for the outer layer was C No. 2, and the most dangerous was C No. 3.

Effect of Plastic Deformation of the Inner Metallic Layer on the Stress-Strain State and Strength of the Outer Composite Layer. In all the above cases of examining the MC cylinders ($0.1 \leq \beta \leq 0.8$), the inner steel layer underwent significant plastic strains. Let us prove it by specific numerical calculations.

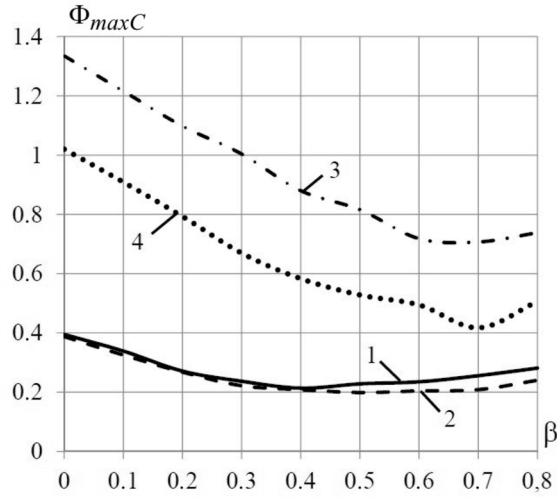


Fig. 1. The Φ_{maxC} vs β for four composites in the outer layers of thin-walled MC cylinders: (1) [St20; C No. 1], (2) [St20; C No. 2], (3) [St20; C No. 3], and (4) [St20; C No. 4].

Denote the maximum radial displacement and circumferential strain by u_{max} and $\varepsilon_{\varphi-max} = (u_{max}/R) \times 100\%$, respectively, of the inner steel layer surface $r = R$ reached at the first half-period of radial vibrations of the MC cylinder. With β from 0.1 to 0.8, the following results for the MC cylinders were obtained:

[St20; C No. 1]: u_{max} monotonically increases from 0.3272 to 0.567 mm, $\varepsilon_{\varphi-max}$ monotonically increases from 0.218 to 0.378%;

[St20; C No. 2]: u_{max} monotonically increases from 0.4293 to 0.6182 mm, $\varepsilon_{\varphi-max}$ monotonically increases from 0.286 to 0.412%;

[St20; C No. 3]: u_{max} monotonically increases at $0.1 \leq \beta \leq 0.3$ from 0.6814 to 0.6868 mm and then at $0.3 \leq \beta \leq 0.8$ monotonically decreases from 0.6868 to 0.6759 mm; $\varepsilon_{\varphi-max}$ monotonically increases at $0.1 \leq \beta \leq 0.3$ from 0.4543 to 0.4579% and then at $0.3 \leq \beta \leq 0.8$ monotonically decreases from 0.4579 to 0.4506%;

[St20; C No. 4]: u_{max} monotonically decreases from 0.7985 to 0.6922 mm, $\varepsilon_{\varphi-max}$ monotonically decreases from 0.5323 to 0.4615%.

The global minimum and maximum of u_{max} (and hence $\varepsilon_{\varphi-max}$ as well) for the MC cylinders are as follows:

$(u_{max})_{min} = 0.3292$ mm and $(\varepsilon_{\varphi-max})_{min} = 0.218\%$ for [St20; C No. 1] at $\beta = 0.1$;

$(u_{max})_{min} = 0.7985$ mm and $(\varepsilon_{\varphi-max})_{min} = 0.5323\%$ for [St20; C No. 4] also at $\beta = 0.1$.

For these two extreme cases at $\beta = 0.1$, Fig. 2 for [St20; C No. 1]) and Fig. 3 for [St20; C No. 4]) are plotted. They depict the time variations of the radial displacement u and circumferential stress σ_{φ} of the inner steel layer surface $r = R$. As is seen, the plastic steel deformation is responsible for a significant difference in the curves, even for the “weakest” case [St20; C No. 1] in terms of the plastic flow (Fig. 2). For [St20; C No. 4], the displacements and strains were almost 2.5 times larger than those in [St20; C No. 1], and the corresponding plots differ much more (Fig. 3). The plastic deformation brings about an increase in u_{max} at the first half-period of radial vibrations, but then their amplitude and frequency become smaller compared to ideally elastic solutions. The reason is that elastoplastic steel is more pliable than ideally elastic, and at the first half-period, when the pressure pulse from the explosion acts on the inner surface, it receives a larger deflection (more precisely, buckling). Starting from the second half-period and further, the explosive loading has practically no effect, but in the elastoplastic layer, the irreversible energy losses for its plastic deformation have managed to occur and, therefore, the vibration amplitude will be smaller than for the ideally elastic case in which there are no energy losses by definition and vibrations occur without damping. As regards σ_{φ} , starting from the first half-period and further in the elastoplastic problem, their amplitude is much smaller than in the ideally

elastic one since for the case of the nonhardening material flow theory [1, 5], the stress intensity can never exceed $\sigma_Y = 250$ MPa.

The global minimum and maximum of the largest deflection (buckling) of the inner surface are reached for the MC cylinders with the thinnest ($\beta = 0.1$) inner steel layer. Therefore, for completeness of examination, Fig. 4 is constructed, similar to Figs. 2 and 3 with the only difference that it corresponds to the MC cylinder [St20; C No. 4] with the thickest ($\beta = 0.8$) of the inner steel layers. At $\beta = 0.8$, this MC shell was most buckled among the four ones: $u_{max} = 0.6922$ mm > 0.6759 mm for [St20; C No. 3] > 0.6122 mm for [St20; C No. 2] > 0.567 mm for [St20; C No. 1].

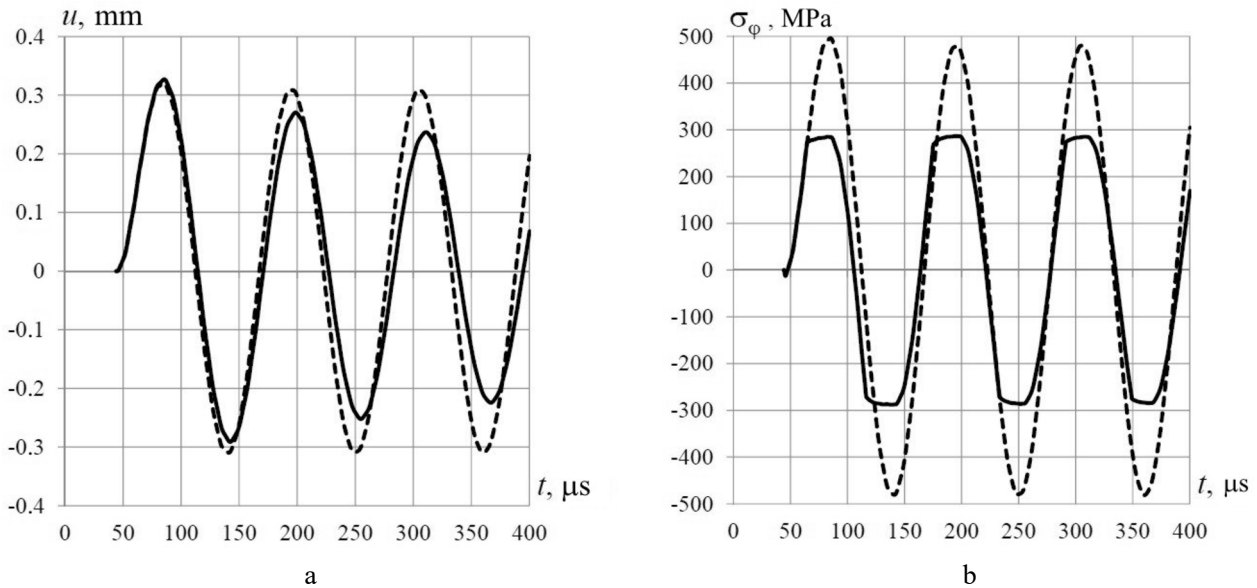


Fig. 2. Variations of $u(t)$ (a) and $\sigma_\varphi(t)$ (b) of the inner surface of the thin-walled MC cylinder [St20; C No. 1] at $\beta = 0.1$. [Here and in Figs. 3, 4, 7, 8, and 9: the solid line corresponds to the elastoplastic inner steel layer ($\sigma_Y = 250$ MPa), and the dashed one corresponds to the case when St20 was considered ideally elastic ($\sigma_Y = \infty$).]

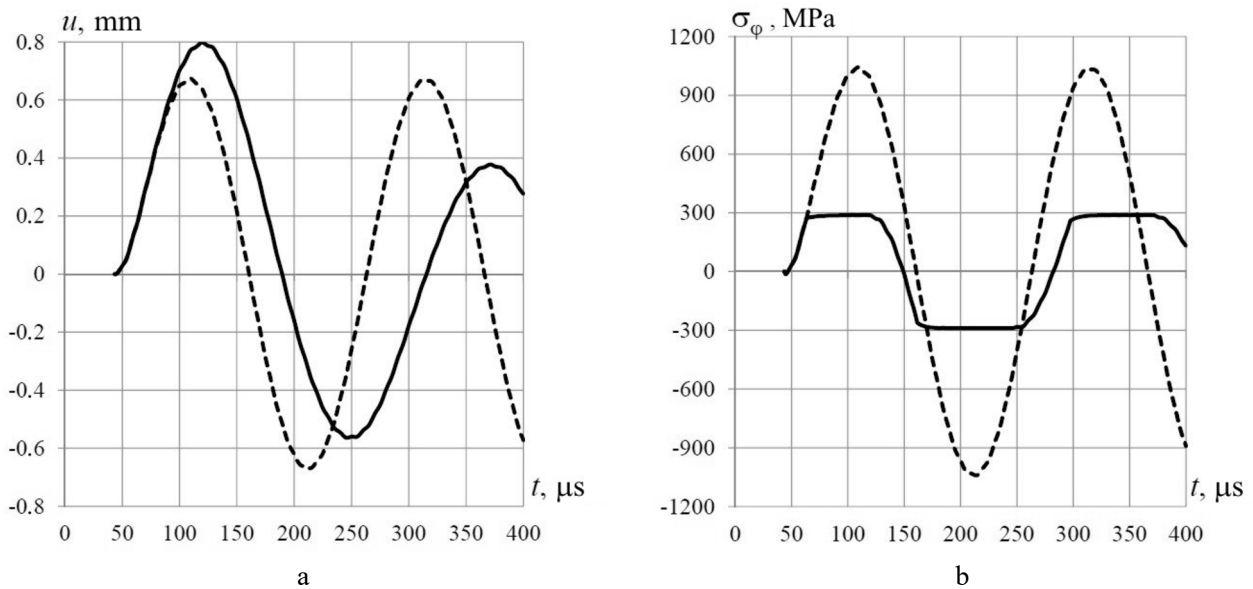


Fig. 3. Variations of $u(t)$ (a) and $\sigma_\varphi(t)$ (b) of the inner surface of the thin-walled MC cylinder [St20; C No. 4] at $\beta = 0.1$.

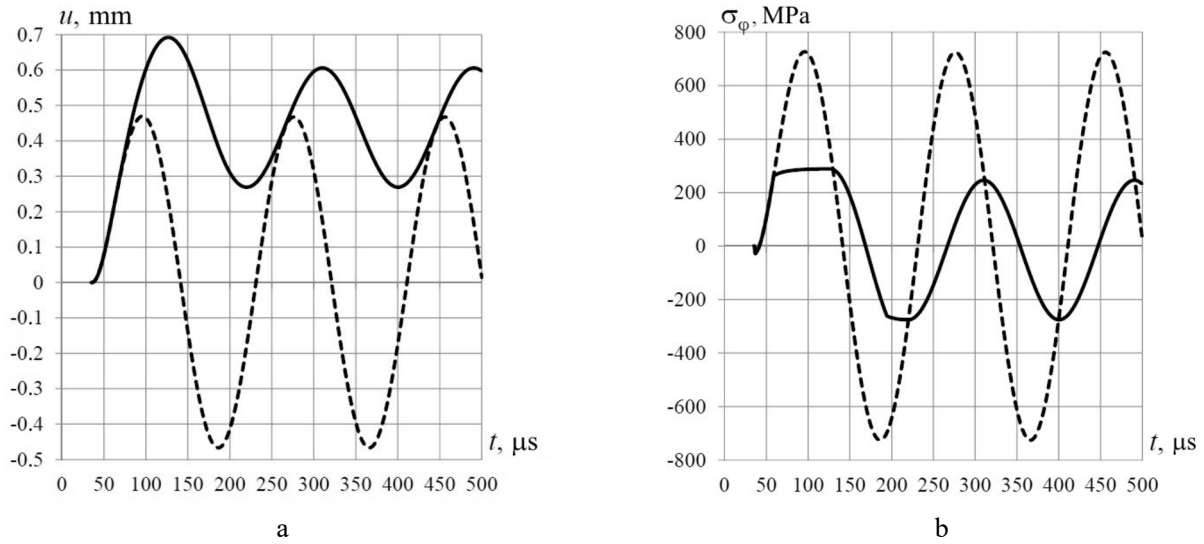


Fig. 4. Variations of $u(t)$ (a) and $\sigma_\varphi(t)$ (b) of the inner surface of the thin-walled MC cylinder [St20; C No. 4] at $\beta = 0.8$.

Figure 4 turned out to be most representative: it clearly shows the residual plastic deflection (buckling) of about 0.44 mm in the elastoplastic formulation around which harmonic vibrations of the shell occur after the drop of loading. Strictly speaking, the residual deflection was also in other elastoplastic formulations, perhaps, somewhat smaller and not so clearly defined.

In conclusion of this discussion, take a look at the effect of plastic deformation of the inner steel layer on the strength of the outer composite one. Let us consider the most durable and the most dangerous MC cylinders in their optima, i.e., at their $\beta = \beta_{opt}$. These are, respectively, MC cylinders [St20; C No. 2] at $\beta = 0.5$, where in the elastoplastic formulation $\Phi_{maxC}(\beta_{opt} = 0.5) = \min = 0.1988$ and [St20; C No. 3] at $\beta = 0.7$, where in the elastoplastic formulation $\Phi_{maxC}(\beta_{opt} = 0.7) = \min = 0.7072$. Time variations of Φ_{maxC} for [St20; C No. 2] at $\beta = 0.5$ and [St20; C No. 3] at $\beta = 0.7$ are shown in Fig. 5.

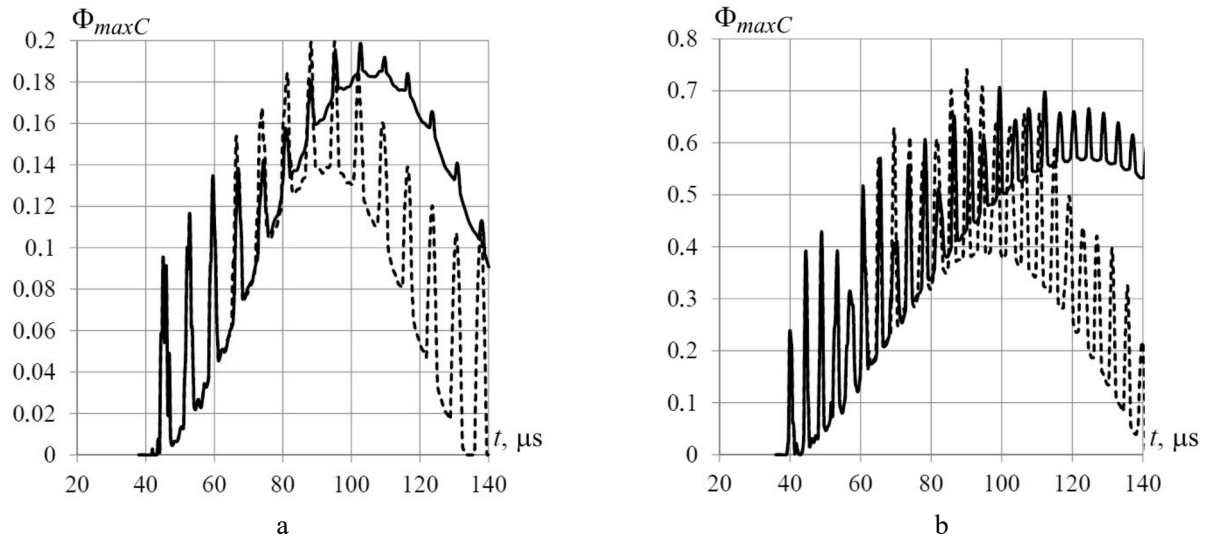


Fig. 5. Variations of $\Phi_{maxC}(t)$ for the optimum thin-walled MC cylinders [St20; C No. 2] (a) and [St20; C No. 3] (b). (Here and in Fig. 10: solid lines are elastoplastic calculation and dashed lines are ideally elastic one.)

The curves of the elastic and elastoplastic calculations qualitatively differ significantly from each other. With this, either the most dangerous points $r = r_{cr}$ or the corresponding critical moments of time $t = t_{cr}$ did not also coincide. The quantitative difference is insignificant:

for [St20; C No. 2] at $\beta = 0.5$, Φ_{maxC} was equal to 0.1988 in the elastoplastic and 0.1996 in the elastic formulations. The relative excess of the elastic calculation over the elastoplastic one equals: $\delta = (0.1996 - 0.1988) \times 100\% / 0.1988 = 0.4024\% < 0.5\%$;

for [St20; C No. 3] at $\beta = 0.7$, Φ_{maxC} was 0.7072 in the elastoplastic and 0.7414 in the elastic formulations. The relative excess of the elastic calculation over the elastoplastic one equals: $\delta = (0.7414 - 0.7072) \times 100\% / 0.7072 = 4.836\% < 5\%$.

Medium-Thickness Cylinders.

Determination of β_{opt} and an Outer Composite Layer of Optimum Strength. Double-layer medium-thickness MC cylinders [St20; C] ($H = 20$ mm; $H/R = 20/150 = 0.1333$) were examined for four outer composite layers and nine β values, from 0 to 0.8 with a step of 0.1 (at $\beta = 0$, we have single-layer composite cylinders). The data obtained were used to plot Fig. 6. The MC cylinders [St20; C No. 1] and [St20; C No. 2] as well as thin-walled cylinders are of higher strength than [St20; C No. 3] and [St20; C No. 4]. Even single-layer ($\beta = 0$) shells [C No. 1] and [C No. 2] possessed quite a high safety margin in contrast to similar [C No. 3] and [C No. 4]. At the same time, if the MC cylinder [St20; C No. 4] started to satisfy the strength condition already at $\beta > 0.27$, [St20; C No. 4] only at $\beta > 0.515$. As before, the MC cylinders [St20; C No. 2] were the most durable, while [St20; C No. 3] were the most dangerous. The MC cylinders [St20; C No. 2] are stronger than [St20; C No. 1] and [St20; C No. 4] are stronger than [St20; C No. 3] for the same reasons as for thin-walled cylinders.

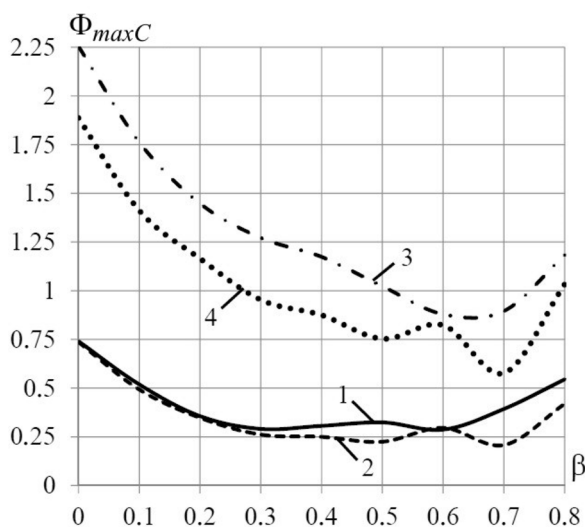


Fig. 6. The Φ_{maxC} vs β for four composites in the outer layers of medium-thickness MC cylinders: (1) [St20; C No. 1], (2) [St20; C No. 2], (3) [St20; C No. 3], and (4) [St20; C No. 4].

From Fig. 6, determine the optimum thickness ratio β_{opt} of the steel layer in which the corresponding Φ_{maxC} are minimum:

for MC cylinder [St20; C No. 1] $\beta_{opt} = 0.6$; $\Phi_{maxC}(\beta_{opt}) = \min = 0.287 \ll 1$;

for [St20; C No. 2] $\beta_{opt} = 0.7$; $\Phi_{maxC}(\beta_{opt}) = \min = 0.2079 \ll 1$;

for [St20; C No. 3] $\beta_{opt} = 0.6$; $\Phi_{maxC}(\beta_{opt}) = \min = 0.8792 < 1$;

for [St20; C No. 4] $\beta_{opt} = 0.7$; $\Phi_{maxC}(\beta_{opt}) = \min = 0.5773 \ll 1$.

The composite of optimum strength for the outer layer was C No. 2, and the most dangerous was C No. 3.

Effect of Plastic Deformation of the Inner Metallic Layer on the Stress-Strain State and Strength of the Outer Composite One. In all the above cases of examining MC cylinders ($0.1 \leq \beta \leq 0.8$), the inner steel layer underwent significant plastic strains. Let us prove this by specific numerical calculations: with β from 0.1 to 0.8, the following results were obtained:

[St20; C No. 1]: u_{max} monotonically grows from 0.3026 to 0.5012 mm; $\varepsilon_{\varphi-max}$ monotonically grows from 0.202 to 0.334%;

[St20; C No. 2]: u_{max} monotonically grows from 0.4067 to 0.5402 mm; $\varepsilon_{\varphi-max}$ monotonically grows from 0.271 to 0.360%;

[St20; C No. 3]: u_{max} monotonically decreases from 0.6289 to 0.5853 mm, $\varepsilon_{\varphi-max}$ monotonically decreases from 0.419 to 0.390%;

[St20; C No. 4]: u_{max} monotonically decreases from 0.7235 to 0.5958 mm, $\varepsilon_{\varphi-max}$ monotonically decreases from 0.482 to 0.397%.

The global minimum and maximum of u_{max} (and hence $\varepsilon_{\varphi-max}$ as well) for all MC cylinders are as follows:

$(u_{max})_{min} = 0.3026$ mm and $(\varepsilon_{\varphi-max})_{min} = 0.202\%$ for [St20; C No. 1] at $\beta = 0.1$;

$(u_{max})_{min} = 0.7235$ mm and $(\varepsilon_{\varphi-max})_{min} = 0.482\%$ for [St20; C No. 4] also at $\beta = 0.1$.

For these two extreme cases at $\beta = 0.1$, Fig. 7 for [St20; C No. 1] and Fig. 8 for [St20; C No. 4] are plotted. They depict the time variations of the radial displacement u and circumferential stress σ_{φ} of the inner steel layer surface $r = R$. As is seen, the plastic steel deformation is responsible for a significant difference in the curves even for the “weakest” case [St20; C No. 1] in terms of the plastic flow (Fig. 7). For [St20; C No. 4], the displacements and strains were almost 2.4 times larger than those in [St20; C No. 1], and the corresponding plots differ much more (Fig. 8). The qualitative effects of plastic deformation of the inner steel layer are the same as those for the thin-walled cylinders.

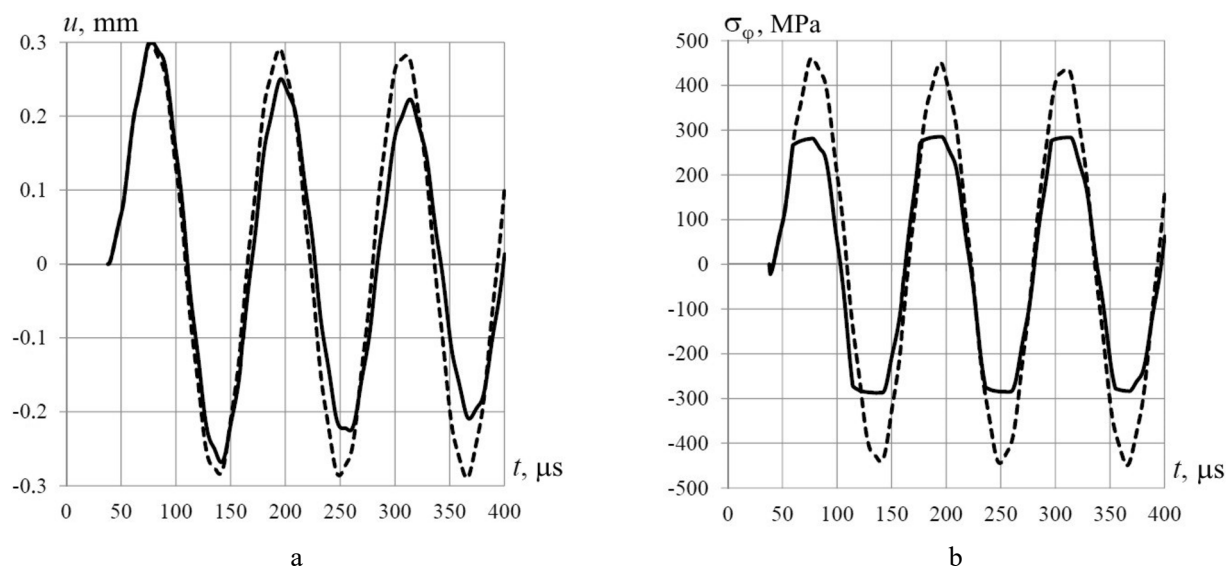


Fig. 7. Variations of $u(t)$ (a) and $\sigma_{\varphi}(t)$ (b) of the inner surface of the medium-thickness MC cylinder [St20; C No. 1] at $\beta = 0.1$.

The global minimum and maximum of the largest inner surface deflection (buckling) are also reached for the MC cylinders with the thinnest ($\beta = 0.1$) inner steel layer. Therefore, for completeness of examination, Fig. 9 is constructed, similar to Figs. 7 and 8 with the only difference that it corresponds to the MC cylinder [St20; C No. 4] with the thickest ($\beta = 0.8$) of the inner steel layers. At $\beta = 0.8$, this MC shell was most buckled among the four ones: $u_{max} = 0.5958$ mm $>$ 0.5853 mm for [St20; C No. 3] $>$ 0.5402 mm for [St20; C No. 2] $>$ 0.5012 mm for [St20; C No. 1].

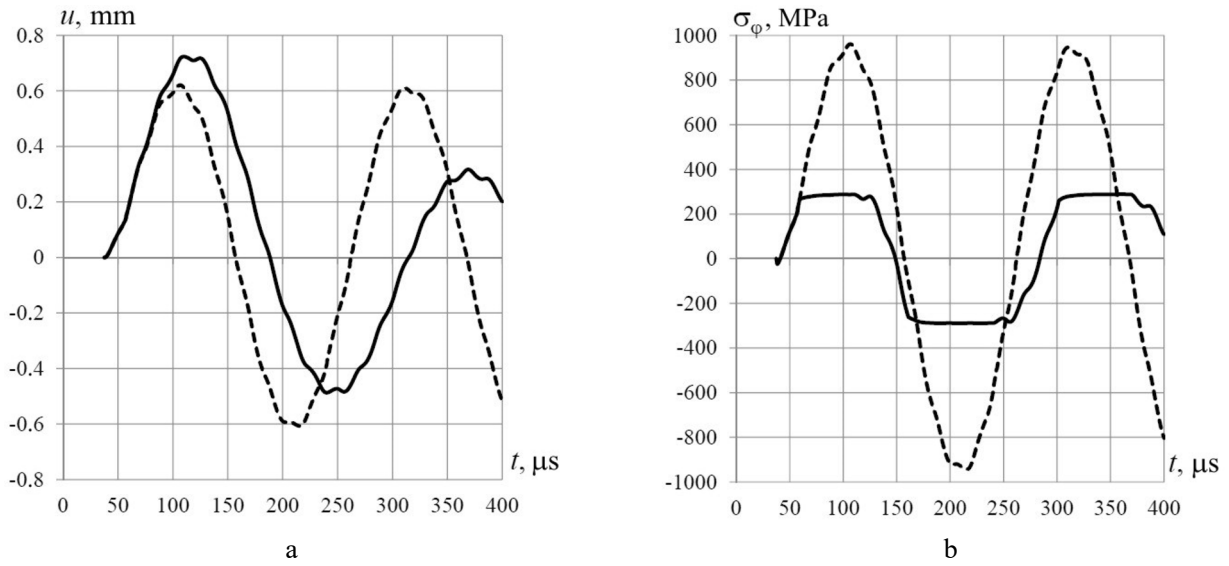


Fig. 8. Variations of $u(t)$ (a) and $\sigma_\varphi(t)$ (b) of the inner surface of the medium-thickness MC cylinder [St20; C No. 4] at $\beta = 0.1$.

As before, Fig. 9 turned out to be most representative: it clearly shows the residual plastic deflection (buckling) of about 0.36 mm in the elastoplastic formulation around which the harmonic vibrations of the shell occur after the drop of loading. Strictly speaking, the residual deflection was also in other elastoplastic formulations, perhaps, somewhat smaller and not so clearly defined.

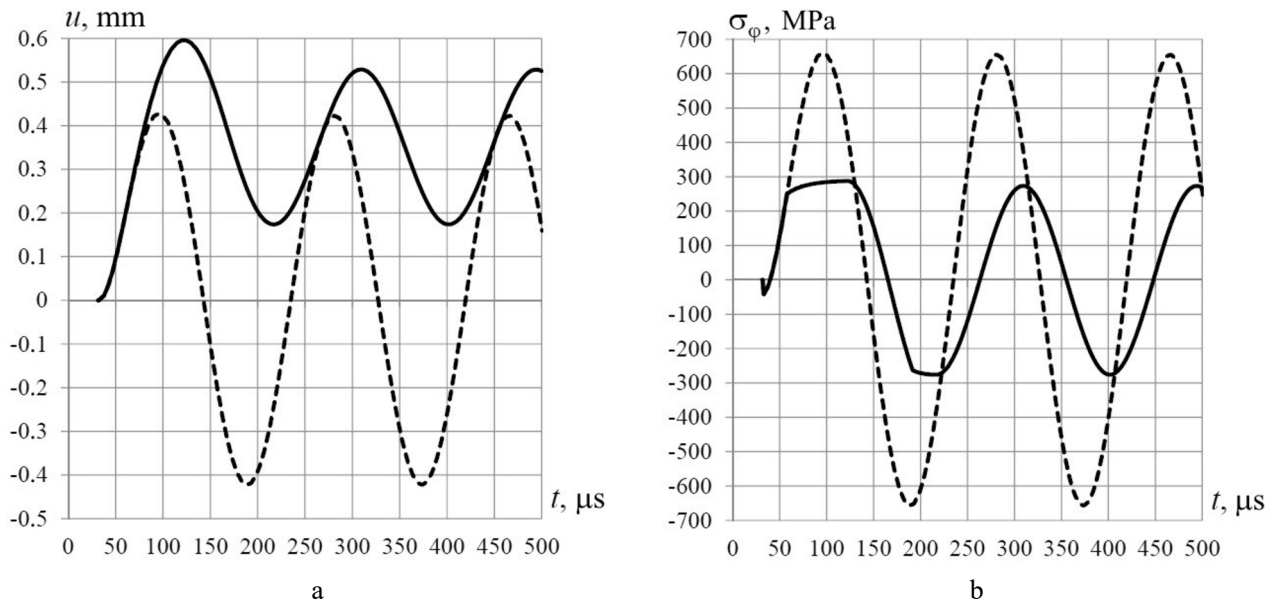


Fig. 9. Variations of $u(t)$ (a) and $\sigma_\varphi(t)$ (b) of the inner surface of the medium-thickness MC cylinder [St20; C No. 4] at $\beta = 0.8$.

In conclusion of this discussion, take a look at the effect of plastic deformation of the inner steel layer on the strength of the outer composite one. Let us consider the most durable and the most dangerous MC cylinders in their optima, i.e., at their $\beta = \beta_{opt}$. These are, respectively, MC cylinders [St20; C No. 2] at $\beta = 0.7$, where in the

elastoplastic formulation, $\Phi_{maxC}(\beta_{opt} = 0.7) = \min = 0.2079$ and [St20; C No. 3] at $\beta = 0.6$, where in the elastoplastic formulation, $\Phi_{maxC}(\beta_{opt} = 0.6) = \min = 0.8792$. Time variations of Φ_{maxC} for [St20; C No. 2] at $\beta = 0.7$ and [St20; C No. 3] at $\beta = 0.6$ are shown in Fig. 10.

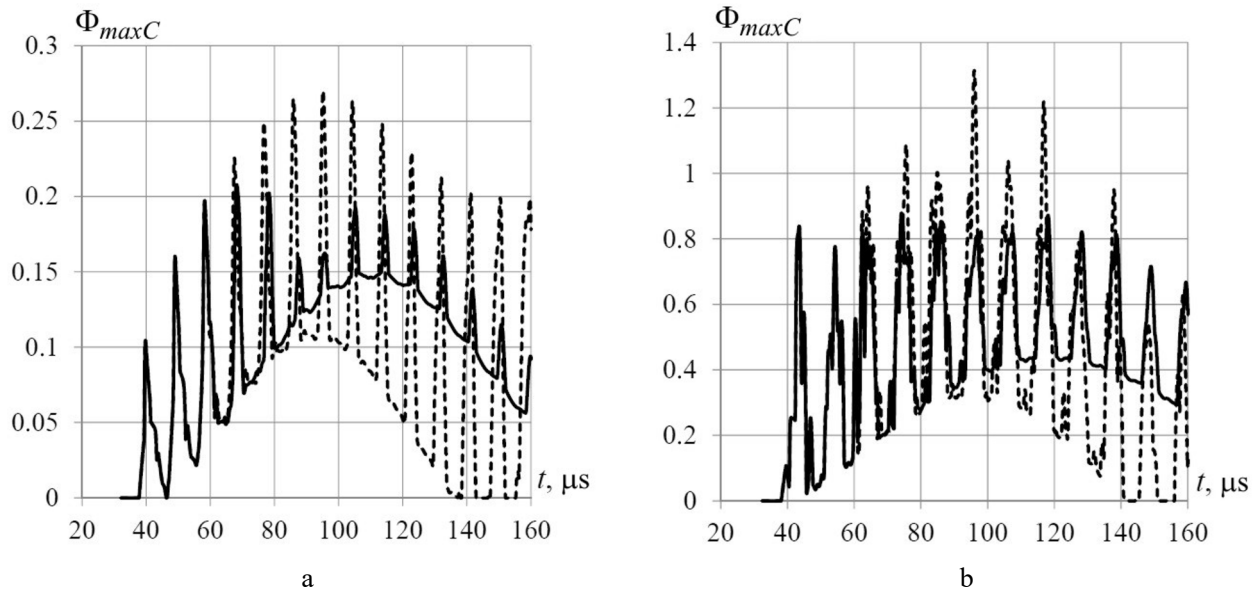


Fig. 10. Variations of $\Phi_{maxC}(t)$ for the optimum medium-thickness MC cylinders [St20; C No. 2] (a) and [St20; C No. 3] (b).

The curves of the elastic and elastoplastic calculations differ significantly from each other both qualitatively and quantitatively. With this, either the most dangerous points $r = r_{cr}$ or the corresponding critical moments of time $t = t_{cr}$ did not also coincide. The quantitative difference in contrast to the thin-walled shells can also be significant:

for [St20; C No. 2] at $\beta = 0.7$, Φ_{maxC} was equal to 0.2079 in the elastoplastic and 0.2702 in the elastic formulations. The relative excess of the elastic calculation over the elastoplastic one equals: $\delta = (0.2702 - 0.2079) \times 100\% / 0.2079 = 30\%$;

for [St20; C No. 3] at $\beta = 0.6$, Φ_{maxC} was 0.8792 in the elastoplastic and 1.314 in the elastic formulations. The relative excess of the elastic calculation over the elastoplastic one equals: $\delta = (1.314 - 0.8792) \times 100\% / 0.8792 = 49.454\% \approx 50\%$.

REFERENCES

1. P. P. Lepikhin, V. A. Romashchenko, O. S. Beiner, and S. O. Tarasovska, "Influence of metal layer thickness on the stress-strain state and strength of metal composite cylinders under internal explosion," *Strength Mater.*, **54**, No. 3, 358–371 (2022). <https://doi.org/10.1007/s11223-022-00411-5>
2. G. Randers-Pehrson and K. A. Bannister, *Airblast Loading Model for Dyna-2D& Dyna-3D*, ARL-TR-1310, Army Research Laboratory (1997).
3. D. W. Hyde, *User's Guide for Microcomputer Program CONWEP, Application of TM5-855-1, Fundamentals of Protective Design for Conventional Weapons* (1992).
4. P. P. Lepikhin and V. A. Romashchenko, *Strength of Inhomogeneous Anisotropic Hollow Cylinders under Impulse Loading* [in Russian], Naukova Dumka, Kiev (2014).
5. N. N. Malinin *Applied Theory of Plasticity and Creep* [in Russian], Mashinostroenie, Moscow (1975).
6. G. S. Pisarenko, A. P. Yakovlev, and V. V. Matveev, *Handbook on Strength of Materials* [in Russian], Delta, Kiev (2008).

7. P. P. Lepikhin, V. A. Romashchenko, O. S. Beiner, et al., “A program for numerical calculation of dynamic stress-strain state and strength of hollow multilayer anisotropic cylinders and spheres. Part 1. Program description,” *Strength Mater.*, **47**, No. 2, 249–256 (2015). <https://doi.org/10.1007/s11223-015-9655-x>
8. M. L. Wilkins, “Calculation of elastic-plastic flows,” in: *Computational Methods in Hydromechanics* [Russian translation], Mir, Moscow (1967).
9. N. K. Naik, Y. Chandra Sekher, and Sailendra Meduri, “Damage in woven-fabric composites subjected to low-velocity impact,” *Compos. Sci. Technol.*, **60**, No. 5, 731–744 (2000).
10. S. G. Lekhnitskii, *Theory of Elasticity of an Anisotropic Body* [in Russian], Nauka, Moscow (1977).